Materials Physics and Mechanics 45 (2020) 87-95 Received: March 11, 2020

NANO- AND MICROPARTICLE AGGREGATION: UNIQUE OPTICAL VECTORS FOR CONTROL

Alexandra G. Bezrukova* **and Olga L. Vlasova**

Institute of Biomedical Systems and Biotechnology, Peter the Great St. Petersburg Polytechnic University

Polytekhnicheskaya 29, St. Petersburg, 195251, Russian Federation

*e-mail: bezr@pb1097.spb.edu

Abstract. The multiparameter analysis of simultaneous optical data for systems of nano- and/or micro-particles (*3D* disperse systems, dispersions, colloids, ensembles with the average diameter less than 10 micrometers) can be presented as the system characteristics characterized by *N*-dimensional unique vectors of optical parameters that can elucidate changes in the state of system particles. The application of *ND* unique optical vector approach is shown for several biomedical dispersions at the processes of aggregation. This approach can serve as the online control platform for the management of technological processes with *3D* disperse systems.

Keywords: absorbance, aggregation, biomedical nano and micro particle, light scattering, *ND* optical vector, *3D* disperse system

1. Introduction

Ensembles of nano- and/or micro- particles can be considered as three-dimensional (*3D*) disperse systems (DS) with particles as a disperse phase in dispersive medium [1]. Many natural particles are declined to form aggregates which state is the problem of control. Multiparameter analysis of optical data for *3D* DS can provide further progress in detailed characterization of *3D* DS. In this analysis the following procedures are included:

- simultaneous measurements of *3D* DS by different compatible nondestructive optical methods such as refractometry, absorbance, fluorescence, light scattering (integral and differential, static and dynamic, unpolarized and polarized), and
- solution of inverse optical problem by different methods and technologies of data interpretation.

Considering the optical theory [1-5] and the results of experiments [6-16] allowed to elaborate so called "unique vector approach" [8,16] as the platform for online control of the processes in *3D* DS. The experience suggests that the set of optical parameters of so-called "second class" (obtained by processing of measured values and independent on the concentration of particles) can be unique for each *3D* DS [8, 16]. In other words, each *3D* DS can be characterized by unique *N*-dimensional vector in the *N*-dimensional space of the second-class optical parameters.

In the unique vector approach after detailed the *3D* DS study, there is refuse from full dispersion characterization in order to obtain information on averaged properties that can be used for solving technological problems. The calculations are based only on experimental data and can be done online.

http://dx.doi.org/10.18720/MPM.4512020_9

2. Materials and methods

Our research [6-16] has studied different *3D* DS with nano- and/or micro- particles (with an average diameter of less than 10 micrometers) and their mixtures [10,14,15]. In this article, some results of aggregation analysis are shown on several examples of biomedical *3D* DS including liposomes, lipoproteins and influenza virus dispersions (strain A1-H1N1) (Fig. 1).

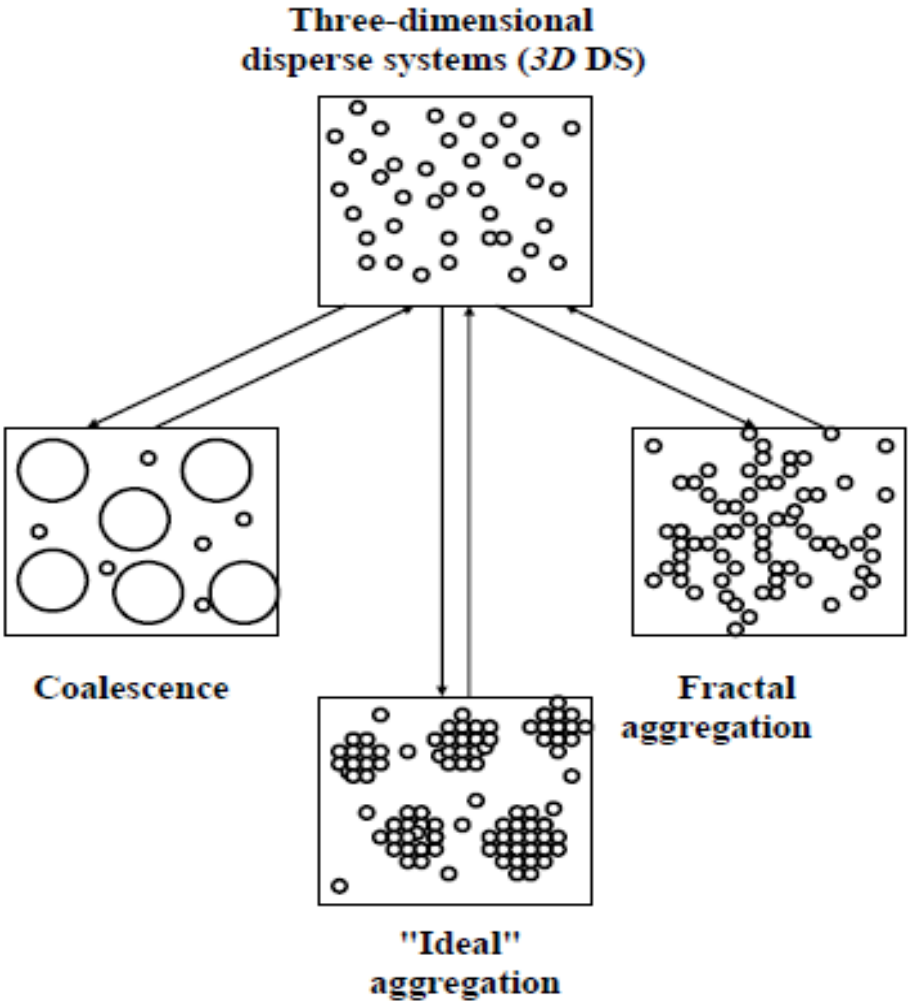

Fig. 1. Scheme of *3D* DS possible aggregation ways

In the previous articles [6-16] there are discussions of the main compatible optical methods for *3D* DS characterization including spectroturbidimetry (ST) [1,5,9] and dynamic light scattering (DLS) [3,9], the *3D* DS polymodality [12], polarization measurements information possibilities [13], inverse optical problems [3,4,14]. The *ND* unique optical vector of *3D* DS [16] is the set of the second-class optical parameters by which the *3D* DS can be characterized and compared with each other *3D* DS. One of the main second-class parameters is "wave exponent" – $n(\lambda)$ [1,5,9], which can be obtained by measuring on spectrophotometers the extinction of light due to integral light scattering (Fig. 2).

For solution of the inverse optical problem of integral light scattering the "turbidity spectrum method" or spectroturbidimetry ST [1,5] can be used. The optical density D and turbidity τ are connected by the equation:

$$\tau = 2.3\, D / l \ , \qquad (1)$$

where l is the length of the optical way (length of cuvette, in cm).

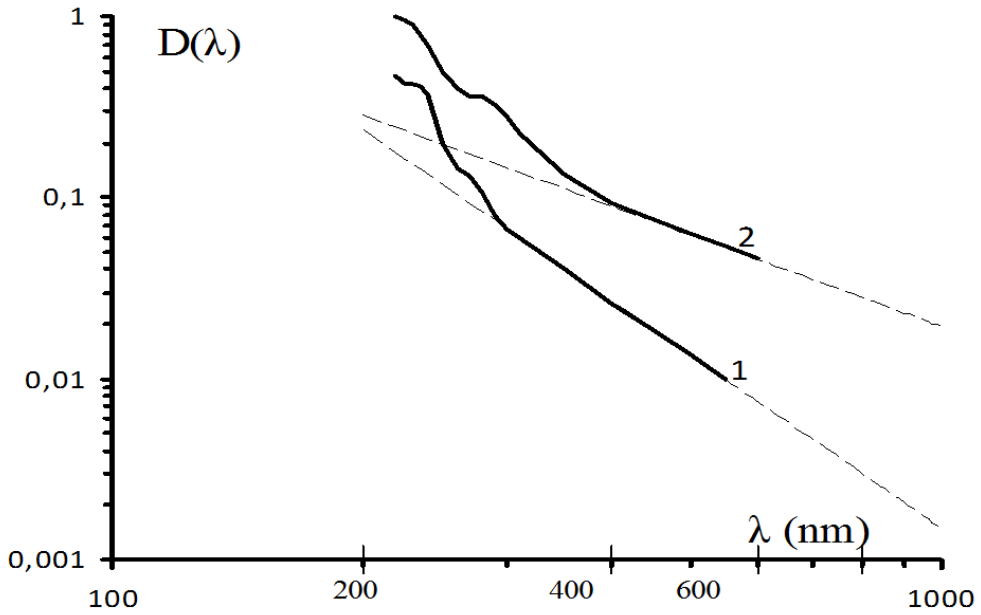

Fig. 2. Bi-logarithmical plot of optical density spectra $D(\lambda)$ as an example of liposomal aggregation at storage. Measurements were made at acceptance angle of photoreceiver (γ) equal to 0.2°. Values of n (500): 1) 3.07 and 2) 1.66. Uncertainty of n (500) is 3%.

At the interval of wavelength (λ), where there is no absorbance of light by *3D* DS (imaginary part of particle refractive index is about zero), the optical density spectra $D(\lambda)$ can be considered as the measure of integral light scattering (except the aperture angle of a photo-receiver). In a bi-logarithmic scale the slope of linear part of $D(\lambda)$ shown in Fig. 2 is $n(\lambda)$ [1,5]:

$$n(\lambda) = -\frac{\Delta\ lg\, D(\lambda)}{\Delta\ lg\, \lambda}. \quad (2)$$

It is necessary to underline that the values of $n(\lambda)$, $D(\lambda)$, parameters of differential light scattering as intensity I (θ, λ) at scattering angle θ, and others are dependent on the acceptance angle of photoreceiver γ (Fig. 3). In all the figures in the text, the results of measurements with γ = 0.2° (due to attached diaphragms) and with other equal conditions are presented.

The function $n(\lambda)$ is the characteristic function with respect to the wavelength size of particles α, and relative to the dispersive medium refractive index of particles m_p [1,5]:

$$\alpha = \frac{\pi\ d\ \mu_m}{\lambda}, \quad (3)$$

$$m_p = \frac{\mu_p}{\mu_m}, \quad (4)$$

where d is the diameter of particles, μ_m and μ_p are the absolute refractive indexes of surrounding dispersive medium and particles, correspondingly. Particle materials are described using their complex refractive index with an imaginary part, but for those wavelengths (usually in the visible region, Fig. 2) where absorbance by particle molecules is absent**,** it is possible to consider only the real part of refractive indexes:

$$m_{ma} = \frac{\mu_{ma}}{\mu_m}, \quad (5)$$

where m_{ma} and μ_{ma} are the relative and absolute refractive indexes of aggregates.

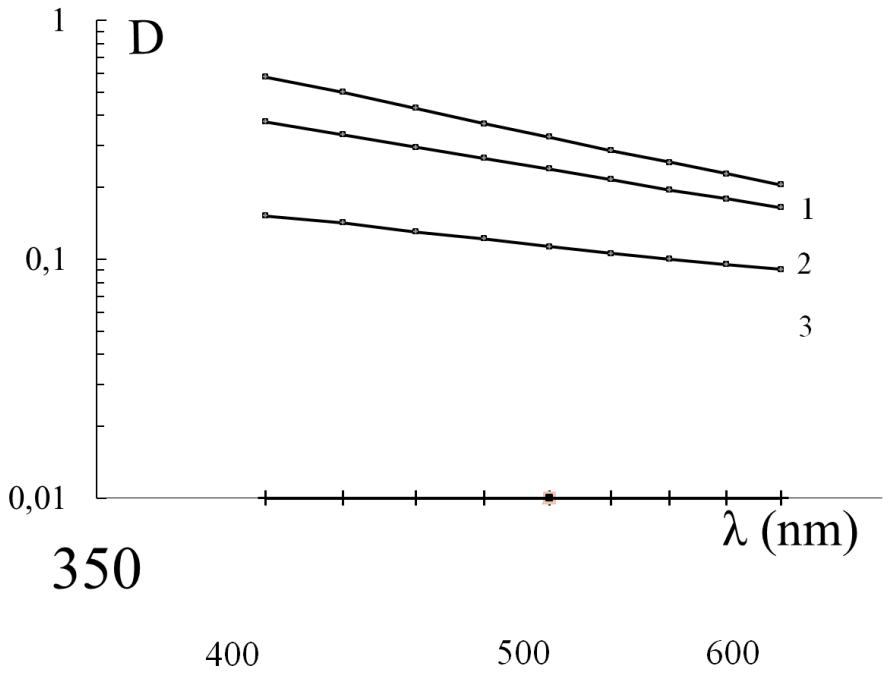

Fig. 3. $D(\lambda)$ dependence on the acceptance angle of photoreceiver (γ) for the same liposomal dispersion (bi-logarithmical plot): 1) γ = 0.2°, n (500) = 2.57, D (500) = 0.325; 2) γ =3.25°, n (500) = 2.04, D (500) = 0.238; 3) γ = 13°, n (500) = 1.27, D (500) = 0.113

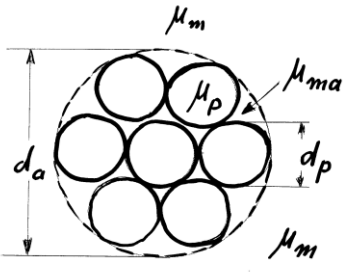

Fig. 4. Scheme of "ideal" aggregate: μ_{ma} can be estimated as averaged by aggregate volume with shares of inner medium and particles

At the coalescence process (Fig. 1, example: fat emulsions) the refractive index of newly formed particles (droplets) can be the same as for initial particles. According to electron microscopy dates, influenza virus and lipoprotein aggregation processes can be discussed as "ideal" and fractal types, correspondingly (Fig. 1).

3. Results and discussion

Natural *3D* DS are polymodal and polycomponent systems [12,14]. Inverse optical problem solution for natural *3D* DS meets with difficulties due to necessity of "a priori" information. Characterization by *ND* vectors can overcome these difficulties. The measurement of $D(\lambda)$ and calculation of $n(\lambda)$ can present the first information about the *3D* DS state. In Fig. 5 the $D(\lambda)$ spectra for initial liposomal dispersion – line 1 with n (500) = 2.34, and for its different diluted portions – lines 2 - 4 with n (500) equal to 2.38, 2.30 and 2.34 correspondingly, are presented. According to preserving in the limits of uncertainty the values of n (500) (slopes in bi-logarithmical scale), the conclusion can be done that the initial dispersion is stable to aggregation.

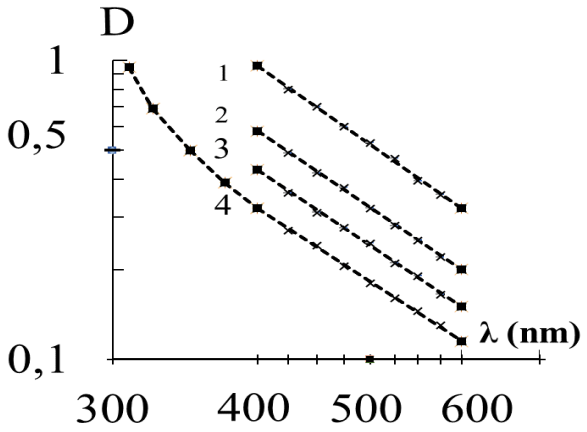

Fig. 5. Bi-logarithmical scale of $D(\lambda)$ for liposomal dispersions with n (500): 1) 2.34; 2) 2.38; 3) 2.30, 4) 2.34. The relative errors of $n(\lambda)$ are 3%. Dispersions N 2 – N 4 were made by dispersion N 1 dilution in buffer for testing its stability to aggregation

Usually $n(\lambda)$ decrease can be considered as the sign of aggregation. Other optical parameters such as $D(\lambda)$, the measure of integral light scattering (out of absorbance band), and I (θ), the measure of differential light scattering, at aggregation can change in different ways for different dispersions (Fig. 6). The particle size distributions in Figs. 7-8 allow explaining the experimental results in Figure 6 by different processes of lipoprotein and influenza nanoparticle aggregation. It is possible to conclude that the unique *ND* vectors for aggregation control of these dispersions should be also different.

In Figure 7 a, the process of lipoprotein aggregation at storage (the first approximation of atherosclerosis model) is presented. Both methods, DLS and ST, allow monitor changes in the state of lipoprotein dispersion. The DLS with regularization algorithm for solving inverse problem allows differentiating not only two main fractions of nano- and micro- particles which diameters differ from each other in about 100 times, but also the bimodal size distribution of nanoparticles. At the analysis by ST, the bimodal or three modal polydisperse size distributions are approximated as monodisperse monomodal size distributions (Figs. 7-8, dashed lines). These results allow concluding that the ST is sensitive to the presence of nanoparticles among microparticles for these *3D* DS and that the changes of optical dates at lipoprotein and influenza virus aggregation processes can be discussed as ‘ideal” and fractal types correspondingly (Fig. 1).

The *ND* optical parameter vector approach (*ND* vector) can be illustrated on the examples of influenza virus dispersions at different states of aggregation (Figs. 9-10).

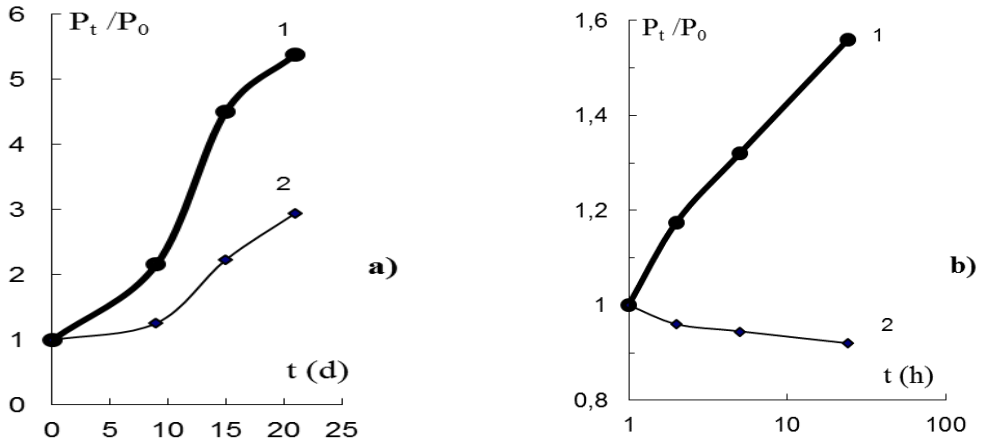

Fig. 6. Examples of *3D* DS optical parameters time (t) dependence - P_t/P_0, during aggregation at ambient condition storage for: a) lipoproteins, t in days – t (d); b) influenza viruses, t in hours – t (h). P_t/P_0: 1) $D_t(\lambda)/D_0(\lambda)$ for a) λ = 700 nm (out of the absorbance spectrum of carotenoids) and for b) λ = 500 nm; 2) ratios of I (θ) at vertical polarization of falling laser light with λ = 633 nm and scattering angle $\theta = 90^o$ – $I_t(90)/I_0(90)$

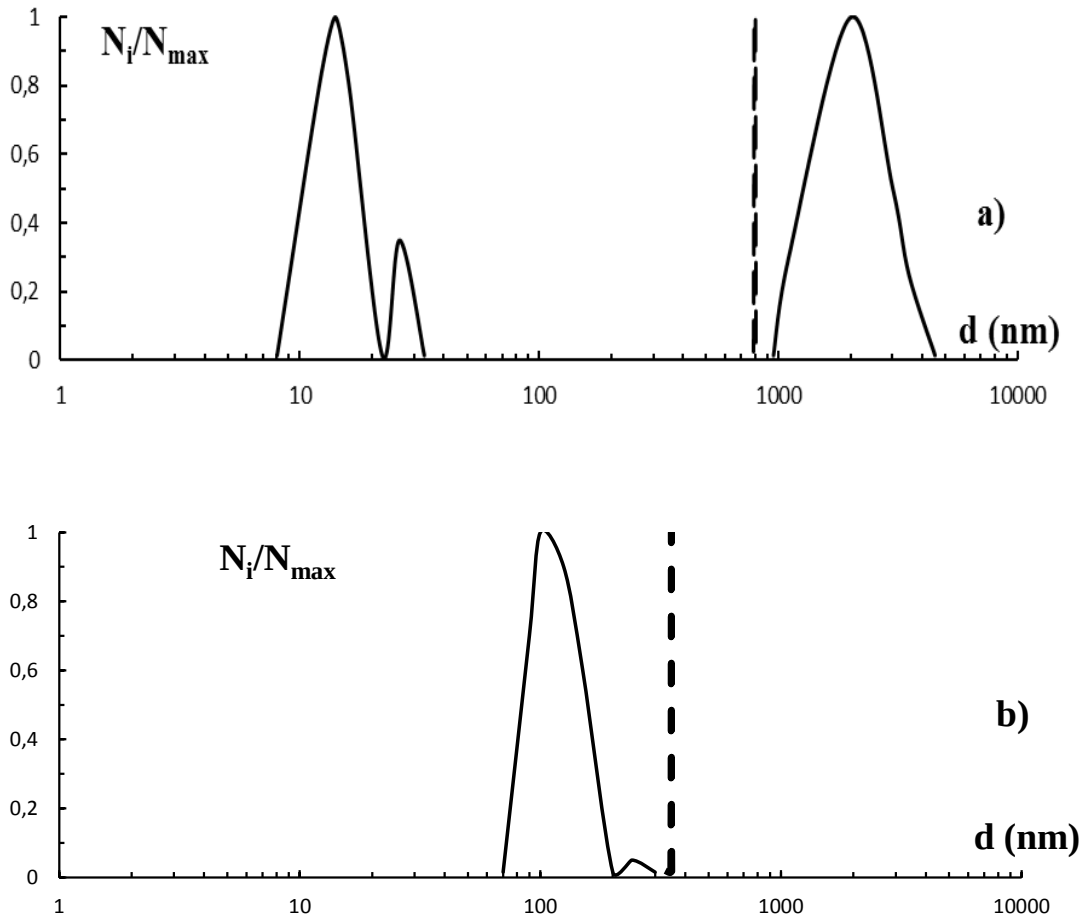

Fig. 7. Lipoprotein (a) and influenza virus (b) aggregated dispersions typical number-size distributions obtained by DLS in the band 500 Hz (solid thin lines) and by ST (dashed lines). For DLS inverse problem solution the regularization algorithm [4] was used

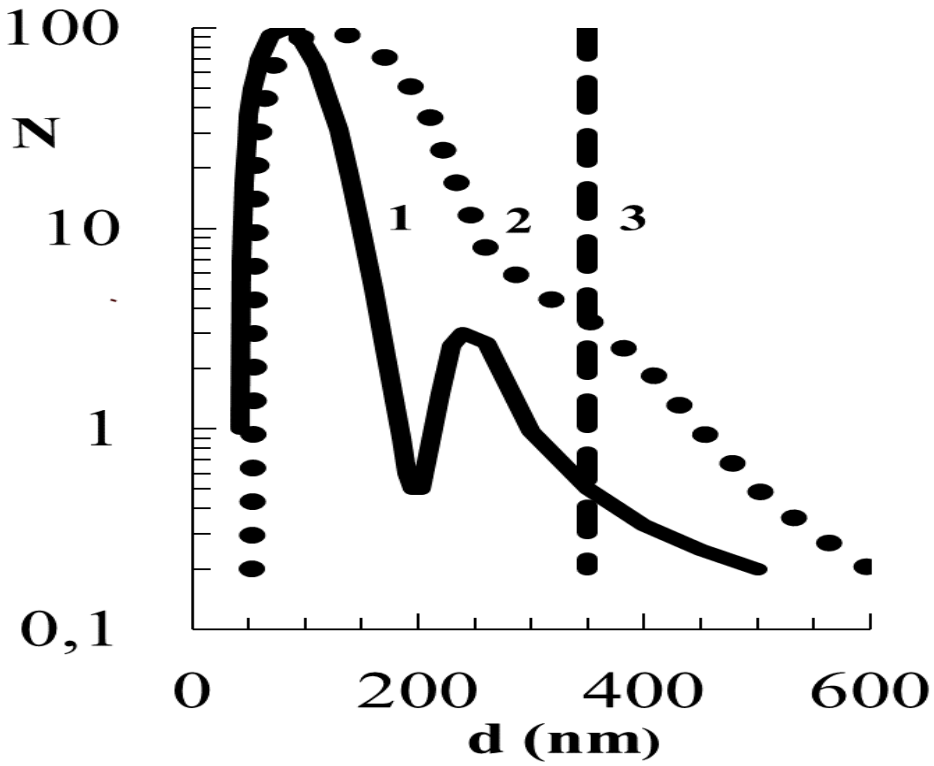

Fig. 8. Number-size distributions for influenza virus aggregated dispersion obtained by inverse optical problem solutions: 1) by DLS with regularization algorithm [4] at the band 500 Hz (as the bimodal size distribution), 2) by DLS at the band 2000 Hz (as monomodal size distribution with the shoulder connected with aggregates) and 3) by ST for the same influenza virus dispersion as the monomodal monodisperse size distribution

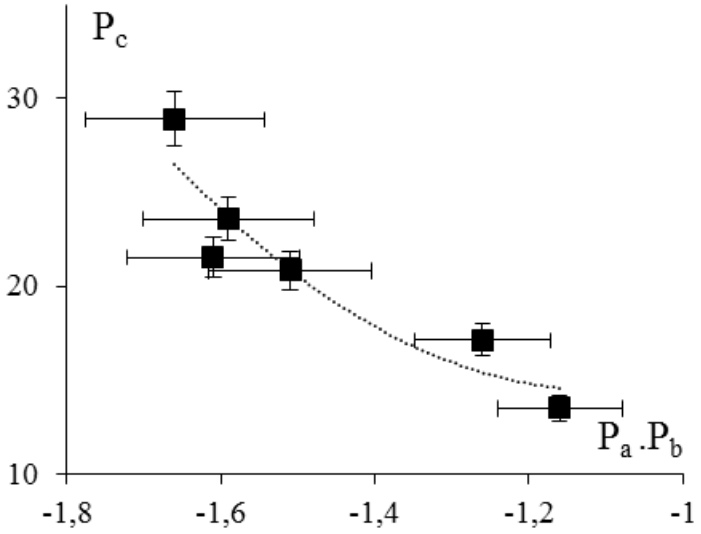

Fig. 9. Presentation on a plane of second-class optical parameter *3D* vectors – **P** {P_a, P_b, P_c} for influenza virus dispersions with a different state of aggregation.
Relative errors for P_a and P_b are 3%, for P_c – 5%. Direction of aggregation is from the left (less aggregated state) to the right (more aggregated state)

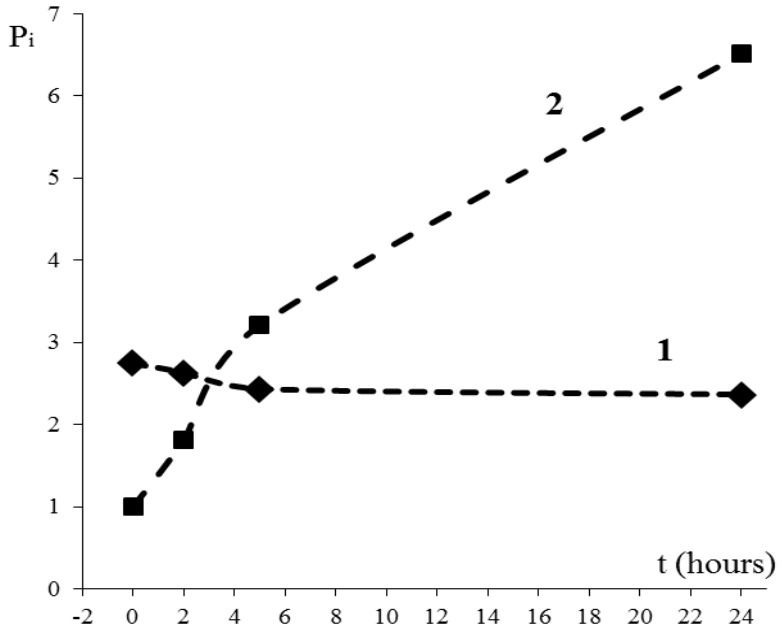

Fig. 10. Time dependence of influenza virus nanoparticles aggregation at ambient conditions storage: **1) $\mathbf{P_i}$** is *1D* vector **$\mathbf{P}_1$** {n (500)}; 2) **$\mathbf{P_i}$** is *7D* vector **$\mathbf{P}_7$** {P_a, P_b, … P_g}. Relative errors for **$\mathbf{P}_1$** {n (500)} and for **$\mathbf{P}_7$** are 3% and 5% correspondingly

In Figure 8 the number-size distributions of influenza virus *3D* DS (obtained by inverse optical problem solutions with regularization algorithm [4] for DLS data at the band 500 Hz) has the bimodal type with the mean hydrodynamic diameter 90 nm for alone virus particles and for aggregates – 240 nm; and at the band 2000 Hz – monomodal type with mean hydrodynamic diameter 120 nm and shoulder at 300 – 400 nm. The inverse optical problem solution by ST for the same virus dispersion presents monomodal monodisperse size distribution with the mean effective equivalent diameter – d = 350 nm corresponding to n (500) = 2.20 and m = 1.17 (model of homogeneous compact aggregation) in the tables of characteristic functions [1, 5]. The effective diameter denotes that the poly-disperse poly-modal *3D* DS size distributions are approximated as a monomodal monodisperse one [1,5]. The equivalent diameter means that the form of particles is approximated as a homogeneous sphere [1,5].

The characterization of influenza virus aggregation process are presented by *3D* vectors **$\mathbf{P_3}$** {P_a, P_b, P_c} in Figure 9 and by *1D* **$\mathbf{P_1}$** {n (500)} and *7D* vectors **$\mathbf{P_7}$** {P_a, P_b, … P_g} in Fig. 10. It can be seen that at ambient conditions storage the influenza virus dispersion state changes from less aggregated: n(500) = 2.7, up to more aggregated state: n (500) = 2.2. The 7*D* vector **$\mathbf{P}_7$** {Pa, Pb, … P g} changes elucidate much more the process of aggregation.

4. Conclusions

ND vector can characterize as unity the *3D* DS state with the minimum interference. Calculations are based only on experimental data (without any models of particle structures and size distributions) and can be done online. For better differentiation of the aggregation state, the number of parameters can be enlarged depending on the *3D* DS specificity. In the unique vector approach after detailed the *3D* DS study, there is the proposal of the optical parameters set which can be a useful tool for online analyzing complex *3D* DS.

Acknowledgements. *Authors thank Prof. Vitaly J. Klenin, Prof. Oleg A. Rosenberg, Dr. Alexander S. Kuznetsov, Prof. Vsevolod M. Kolikov, Prof. Ludmila M. Molodkina, Dr. Tatyana G. Braginskaya, Prof. Vladimir V. Klubin, Prof. Heinrich Hofmann for the help in experiments and useful discussions. No external funding was received for this study.*

References

[1] Klenin VJ. *Thermodynamics of systems containing flexible chain polymers*. Elsevier; 1999.
[2] Mishchenko MI, Hovenier JW, Travis LD. *Light scattering by nonspherical particles: theory, measurements and applications.* AP; 1999.
[3] Braginskaya TG, Dobichin PD, Ivanova MA, Klyubin VV, Lomakin AV, Noskin VA, Shmelev GE, Tolpina SP. Analysis of the polydispersity by photon correlation spectroscopy: regularization procedure. *Physica Scripta*. 1983;28(1): 73-84.
[4] Schnablegger H, Glatter O. Optical sizing of small colloidal particles: an optimized regularization technique. *Applied Optics:* 1991;30(33): 4889-4896.
[5] Shchyogolev SY. Inverse problems of spectroturbidimetry of biological disperse systems: an overview. *Journal of Biomedical Optics*. 1999;4(4): 490-503.
[6] Bezrukova AG. Development of multiparametric optical assay for on-line environmental control, *Proceedings of SPIE - The International Society for Optical Engineering*. 1997;3107: 298-303.
[7] Bezrukova AG. Optical characterization of biological and other systems. *Material Research Society Proceedings.* 2002;711: FF7.9.
[8] Bezrukova AG. Nondestructive testing of *3D* disperse systems with micro- and nano-particles: *N*-dimensional space of optical parameters. *Proceedings of SPIE - The International Society for Optical Engineering*. 2006;62530C: 1-5.
[9] Bezrukova AG, Lubomska M, Magri P, Rogalski M. Differential dynamic and integral static light scattering for nondestructive testing of *3D* disperse systems with nanoparticles. *Proceedings of SPIE - The International Society for Optical Engineering*. 2007;65970M: 1-7.
[10] Bezrukova AG, Lubomska M, Rogalski M. Nanoparticle mixtures of anthracene and β-cyclodextrin testing by optical spectroscopy. *Reviews on Advanced Materials Science*. 2009;20(1): 70-76.
[11] Bezrukova AG. Nanoparticle interactions: improvement of experimental optical data analysis. *Proceedings of SPIE - The International Society for Optical Engineering*. 2009;73770B: 1-7.
[12] Bezrukova AG, Vlasova OL. Optical characterization of *3D* disperse systems with nano- and micro- particles: polymodality of size distributions. *Materials Physics and Mechanics.* 2012;13(2): 162-174.
[13] Bezrukova AG, Vlasova OL. Optical characterization of *3D* disperse systems with nano- and micro- particles: light scattering matrix elements. *Materials Physics and Mechanics.* 2014;20(2): 124-129.
[14] Bezrukova AG, Vlasova OL. Mixtures of *3D* disperse systems with nano- and micro-particles: Optical characterization. *St. Petersburg Polytechnic University Journal, Physics and Mathematics.* 2016;2(4): 316-321.
[15] Bezrukova AG. Characterization of biomedical nanoparticles mixtures as N-dimensional optical parameter vectors for on-line control. *European Cells and Materials.* 2016;32(Suppl. 5): 89.
[16] Bezrukova AG, Vlasova OL. Optical characterization of *3D* disperse systems with nano- and micro- particles: Unique vectors. *Materials Physics and Mechanics*. 2018;39(1): 81-86.